Journal of Power Sources 194 (2009) 502–507

Contents lists available at ScienceDirect

Journal of Power Sources

journal homepage: www.elsevier.com/locate/jpowsour

Properties of the lithium and graphite–lithium anodes in *N*-methyl-*N*-propylpyrrolidinium bis(trifluoromethanesulfonyl)imide

Andrzej Lewandowski*, Agnieszka Świderska-Mocek

Faculty of Chemical Technology, Poznań University of Technology, PL-60 965 Poznań, Poland

ARTICLE INFO

Article history:
Received 13 October 2008
Received in revised form 28 April 2009
Accepted 15 May 2009
Available online 22 May 2009

Keywords:
Lithium-ion battery
Ionic liquid
N-methyl-*N*-propylpyrrolidinium
bis(trifluoromethanesulfonyl)imide

ABSTRACT

The ternary $[Li^+]_{0.09}[MePrPyr^+]_{0.41}[NTf_2^-]_{0.50}$ room temperature ionic liquid was obtained by dissolution of solid lithium bis(trifluoromethanesulfonyl)imide ($LiNTf_2$) in liquid *N*-methyl-*N*-propylpyrrolidinium bis(trifluoromethanesulfonyl)imide ($[MePrPyr^+][NTf_2^-]$), and studied as an electrolyte for lithium-ion batteries. The graphite–lithium (C_6Li) anode, working together with vinylene carbonate as an additive showed ca. 90% of its initial discharge capacity after 50 cycles. The addition of vinylene carbonate to the neat ionic liquid results in the formation of the protective coating (SEI) on both the lithium and graphite anodes. The SEI formation increases the rate of the charge transfer reaction as well as protects the anode from chemical passivation (corrosion). The graphite–lithium (C_6Li) anode shows good cyclability and Coulombic efficiency in the presence of 10 wt.% of vinylene carbonate as an additive to the ionic liquid.

1. Introduction

Graphite is now the most popular anode material for lithium-ion batteries, used instead of metallic lithium, while the most popular cathodes are based on LiM_xO_y spinell-type oxides, where M = Mn or Co [1,2]. The electrolyte is usually a lithium salt ($LiPF_6$) solution in a mixture of carbonates. A polymer electrolyte, obtained by dissolution of a lithium salt in a polymer network, or the polymer network swollen in a solution of the lithium salt in an organic solvent (gel-type polymer electrolyte) may also be applied [3]. The solvent-free polymer electrolyte is non-volatile, and hence non-flammable, however, its conductivity is low. Instead of a solid salt solution in volatile molecular liquid, non-volatile molten salts may be applied as an electrolyte. Salts liquid at room temperature, usually called room temperature ionic liquids (RTIL), or simply ionic liquids (IL), have been prepared and used as solvents and electrolytes in electrochemical capacitors and in lithium-ion batteries [4,5]. Most low-melting-point salts are quaternary ammonium salts, showing negligible vapour pressure and a broad electrochemical stability [4]. After dissolution of a lithium LiX salt, solid in room temperature, in an ionic liquid $[A^+][X^-]$ (where A^+ is a quaternary ammonium cation), a new ternary $[Li^+]_m[A^+]_n[X^-]_z$ ionic liquid is formed. During the last few years there has been increasing interest in such $[Li^+]_m[A^+]_n[X^-]_z$ ionic liquids as electrolytes for primary lithium batteries or secondary lithium-ion batteries [6–59], due to their non-volatility and hence, non-flammability. An ionic liquid based on *N*-butyl-*N*-ethylpyrrolidinium bis(trifluoromethanesulfonyl)imide $[BuEtPyr^+][NTf_2^-]$, was tested as an electrolyte compatible with the lithium iron phosphate cathode, $LiFePO_4$ [52]. The present paper reports properties of the lithium–graphite anode working together with a room temperature ionic liquid, obtained by dissolving solid lithium bis(trifluoromethanesulfonyl)imide, $LiNTf_2$, in liquid *N*-methyl-*N*-propylpyrrolidinium bis(trifluoromethanesulfonyl)imide $[MePrPyr^+][NTf_2^-]$, with the formation of the ternary $[Li^+]_m[MePrPyr^+]_n[NTf_2^-]_z$ system.

2. Experimental

2.1. Materials

Acetonitrile (Aldrich) was distilled and kept over A3 molecular sieves. Cryptand 222 (4,7,13,16,21,24-hexaoxa-1,10-diazabicyclo[8.8.8]hexacosane, Merck), graphite SL-20 (G, Superior Graphite, USA), carbon black (CB, Fluka), poly(vinylidene fluoride) (PVdF, Fluka), lithium foil (Aldrich, 0.75 mm thick) and lithium bis(trifluoromethanesulfonyl)imide ($LiNTf_2$, Fluka) were used as purchased. *N*-methyl-*N*-propylpyrroldinium bromide ($[MePrPyr^+][Br^-]$) was

Abbreviations: RTIL, room temperature ionic liquid; IL, ionic liquid; $MePrPyr^+$, *N*-methyl-*N*-propylpyrrolidinium cation; $MePrPip^+$, *N*-methyl-*N*-propylpiperidinium cation; NTf_2^-, bis(trifluoromethanesulfonyl)imide anion ($^-N(CF_3SO_2)_2$); VC, vinylene carbonate; CB, carbon black; G, graphite; GC, glassy carbon; PVdF, poly(vinylidene fluoride); Cryptand 222, 4,7,13,16,21,24-hexaoxa-1,10-diazabicyclo[8.8.8]hexacosane; Ag/(Ag^+222, AN), cryptate reference electrode.

* Corresponding author. Tel.: +48 61 6653 309; fax: +48 61 6653 571.
E-mail address: andrzej.lewandowski@put.poznan.pl (A. Lewandowski).

0378-7753/$ – see front matter © 2009 Elsevier B.V. All rights reserved.
doi:10.1016/j.jpowsour.2009.05.029

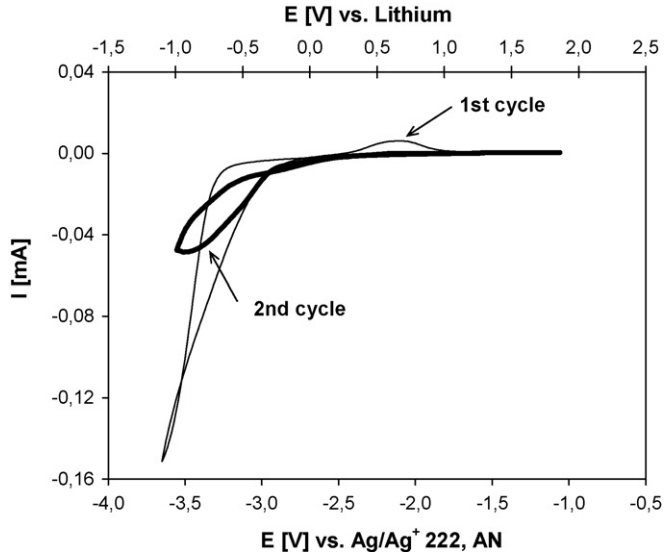

Fig. 1. Cyclic voltamperometry in 0.7 M $LiNTf_2$ in $MePrPyrNTf_2$. Working electrode: glassy carbon (0.070 cm^2), counter electrode: Pt (2 cm^2), reference electrode: Ag/Ag^+222 in AN. Scan rate: 10 mV/s.

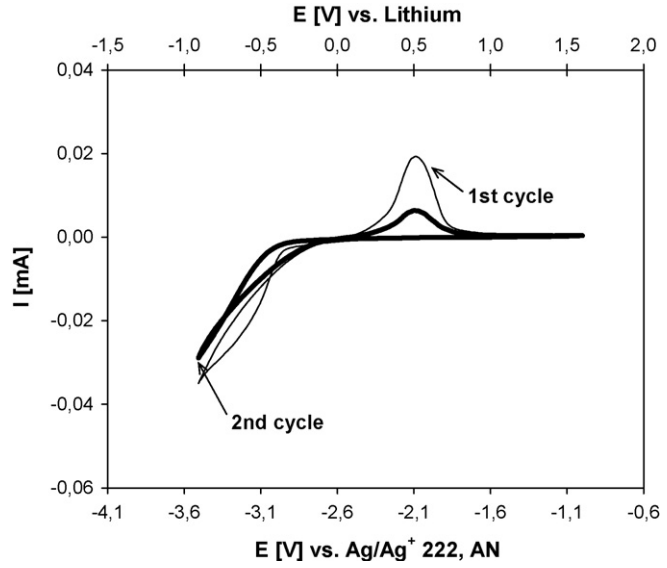

Fig. 2. Cyclic voltamperometry in 0.7 M $LiNTf_2$ in $MePrPyrNTf_2$ containing 10 wt.% VC. Working electrode: glassy carbon (0.070 cm^2), counter electrode: Pt (2 cm^2), reference electrode: Ag/Ag^+222 in AN. Scan rate: 10 mV/s.

obtained from *N*-methylpyrrolidinium (Aldrich) and bromopropane (Aldrich) in acetonitrile. After acetonitrile evaporation white crystals were dissolved in 2-propanol (P.O.Ch., Poland) and after the addition of tetrahydrofurane (P.O.Ch., Poland) white crystals of $[MePrPyr^+][Br^-]$ were precipitated. *N*-methyl-*N*-propylpyrrolidinium bis(trifluoromethanesulfonyl)imide ($[MePrPyr^+][NTf_2^-]$) was obtained from $[MePrPyr^+][Br^-]$ by metathesis with lithium bis(trifluoromethanesulfonyl)imide in aqueous medium. The ionic liquid was dried by evaporation in a vacuum at 50 °C for 10 h. The solid $LiNTf_2$ salt was dissolved in the liquid salt $[MePrPyr^+][NTf_2^-]$ (0.7 M solution of $LiNTf_2$ in $[MePrPyr^+][NTf_2^-]$) to give the Li^+ containing ionic liquid $[Li^+]_m[MePrPyr^+]_n[NTf_2^-]_z$. The water content in the $[Li^+]_m[MePrPyr^+]_n[NTf_2^-]_z$ electrolyte, analyzed with a standard Karl–Fisher titrant (Aldrich), was below the level of 0.4 mg $H_2O\,L^{-1}$. Tested carbon electrodes were prepared on a copper foil (Hohsen, Japan) by the casting technique, from a slurry of the graphite (G), carbon black (CB) and PVdF in *N*-methyl-2-pyrrolidone (NMP, Fluka). The ratio of components (G):(CB):(PVdF) was at the level of 85:5:10 (by weight). After solvent (NMP) evaporation at 120 °C in a vacuum, a layer of the carbon electrode, containing the active material (G), electronic conductor (CB) and the binder (PVdF) was formed.

2.2. Measurements

Cyclic voltammetry curves were recorded with the μAutolab electrochemical system (EcoChemie, the Netherlands). The working glassy carbon electrode (Mineral, Poland) had a surface of 0.070 cm^2. The reference electrode was prepared by placing an Ag wire into a solution of $AgNTf_2$ (0.01 M) and cryptand 222 (0.1 M) in acetonitrile (Ag/Ag^+222, AN reference). The tube, obtained from a conventional calomel electrodes producer (Euro-Sensor, Poland) contained the reference electrode inner solution (Ag^+ 0.01 M + cryptand 222 0.1 M in AN). The Ag/Ag^+222 cryptate reference electrode shows much stable and reproducible potential in comparison to the Ag/Ag^+ reference [60]. Platinum foil (2 cm^2) served as a counter electrode. Density of electrolytes was measured with an Anton Paar DMA 35N meter. Flash point was measured with an open cup home-made apparatus, based on the Cleveland open cup instrument, with a 1.5 ml cup. The cup was heated electrically through a sand bath, and temperature was measured with the M-3850 (Metex, Korea) digital termometer. The apparatus was scaled with a number of compounds of known flash points. The flash point of the $[Li^+]_{0.09}[MePrPyr^+]_{0.41}[NTf_2^-]_{0.50}$ electrolyte has been estimated to be above the decomposition temperature of the $[MePrPyr^+][NTf_2^-]$ salt (>417 °C).

The lithium–graphite electrode was tested for the cycling efficiency against the lithium foil (a counter electrode of the specific charge capacity much higher in comparison to the tested electrode), separated by the glass micro-fibre GF/A separator (Whatman). The Li/electrolyte/Li as well as G + CB + PVdF/electrolyte/Li cells were assembled in an adapted 0.5″ Swagelok® connecting tube in a

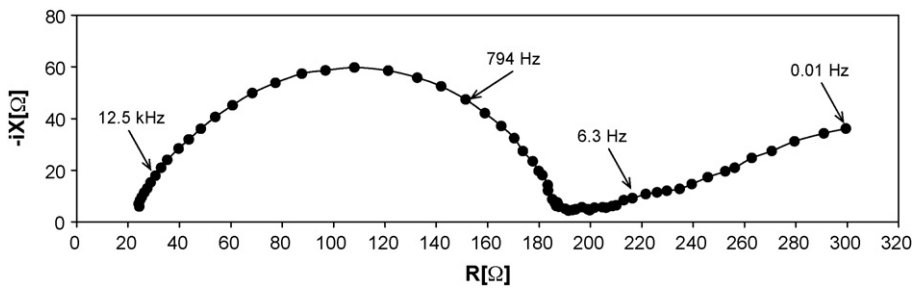

Fig. 3. Impedance plot for the fresh symmetric Li|0.7 M $LiNTf_2$ in $MePrPyrNTf_2$|Li system.

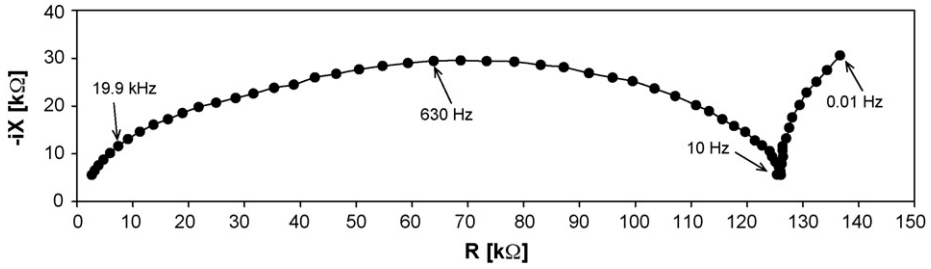

Fig. 4. Impedance plot for the symmetric Li|0.7 M $LiNTf_2$ in $MePrPyrNTf_2$ |Li system recorded after 36 days.

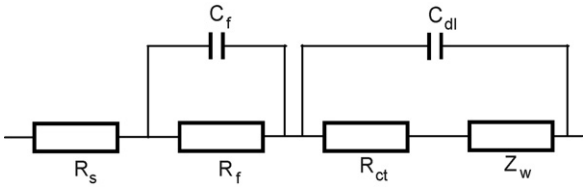

Fig. 5. Equivalent circuit representing analyzed systems.

dry argon atmosphere in a glove box. Charging/discharging of the cell was done at a constant current density of 10 mA g^{-1} of graphite (which is equivalent to the 0.03C rate) with the use of the ATLAS 0461MBI multichannel electrochemical system (Atlas-Sollich, Poland). The potential of the lithium metal being in contact with the ionic liquid was measured against the cryptate reference electrode using the Swagelok® connecting tube. The potential was stabilized after ca. 1 h and was recorded after 2 h.

3. Results and discussion

3.1. $[Li^+][MePrPyr^+][NTf_2^-]$ electrolyte composition

The solubility of the solid lithium-containing salt in the room temperature liquid salt was at the level of ca. 1.54 g of $LiNTf_2$ in 10 g of $[MePrPyr^+][NTf_2^-]$ at room temperature. The resulting ionic liquid had a density of ca. 1.479 g cm^{-3}, the $LiNTf_2$ concentration of ca. 0.7 M and the composition of $[Li^+]_{0.09}[MePrPyr^+]_{0.41}[NTf_2^-]_{0.50}$. At a higher Li^+ content, the system showed a tendency to form a crystalline solid phase. The content of lithium-ion in this ionic liquid is high in comparison to a corresponding system obtained by dissolution of solid $LiNTf_2$ salt in liquid $[MePrPip^+][NTf_2^-]$, which results in a ternary $[Li^+]_{0.04}[MePrPip^+]_{0.73}[NTf_2^-]_{0.23}$ ionic liquid [41]. Even in comparison to classical solutions of lithium salts in organic solvents, the $[Li^+]_{0.09}[MePrPyr^+]_{0.41}[NTf_2^-]_{0.50}$ ionic liquid contains a comparable mole fraction of the lithium cation, or even higher, if expressed vs. the total amount of the electrolyte. For example, the 1 M $LiPF_6$ solution in the mixture of DMC (dimethyl carbonate) and EC (ethylene carbonate), has a density of ca. 1.282 g cm^{-3}, and the composition $[Li^+]_{0.07}[PF_6^-]_{0.07}[DMC]_{0.43}[EC]_{0.43}$ [41].

3.2. Voltamperometry

Fig. 1 shows the cyclic voltamperometric curve for the GC/$[Li^+][MePrPyr^+][NTf_2^-]$ system (without any additive to the ionic liquid electrolyte). At the first cycle, the reduction of the lithium cation on the GC electrode occurs at potentials more negative than 3 V (vs. the Ag/Ag^+222, AN reference). At the reverse scan a peak of lithium oxidation to Li^+ can be seen. However, the corresponding anodic peak does not appear at the second scan. This effect may be caused by the passivation of the tested GC anode; the layer formed at the GC/electrolyte interface does not undergo anodic dissolution. Fig. 2 illustrates voltamperometric curves for the glassy carbon anode with the $[Li^+][MePrPyr^+][NTf_2^-]$ electrolyte containing 10 wt.% of VC as the additive. In this case, in contrast to the latter system, the anodic peak can be seen for both initial as well as the second cycle. This suggests that during the first scan a lithium-cation conducting-film was formed, protecting the carbon/electrolyte interface.

The carbon electrode usually works together with 'classical' solutions of lithium salts in a mixture of cyclic carbonates, which forms an SEI protective coating. In the case of ionic liquids, the use of additives, such as carbonates, is one of the most effective ways of SEI formation. In some cases cyclic carbonates are not as effective in SEI formation. For example, the intercalation of lithium from the electrolyte $[Li^+]_m[EtMeIm^+]_n[NTf_2^-]_{m+n}$ into the graphite was examined [9]. The reduction of the electrolyte (probably of the $[EtMeIm^+]$ cation) without intercalation of lithium into the graphite was observed. After the addition of 25% of ethylene carbonate no protective film was formed, while 2% of acrylonitrile, 5% of ethylene sulphite or 10% of vinylene carbonate led to SEI formation and cycling curves close to those typical of 'classical' electrolytes in cyclic carbonates. Vinylene carbonate has been applied successfully as a SEI forming compound in the case of some other ionic liquids [12,15,28,41].

3.3. Impedance spectroscopy

The formation of the passive layer at the Li/IL interface is suggested by impedance measurements. Fig. 3 shows the impedance spectrum of the symmetric Li/$[Li^+][MePrPyr^+][NTf_2^-]$/Li system,

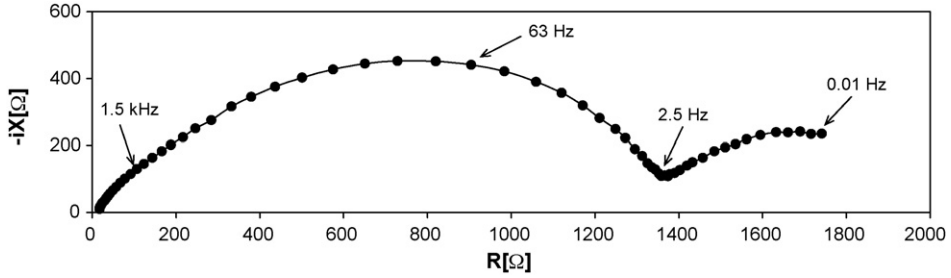

Fig. 6. Impedance plot for the symmetric Li|0.7 M $LiNTf_2$ in $MePrPyrNTf_2$ + 10 wt.% VC|Li system recorded after 34 days.

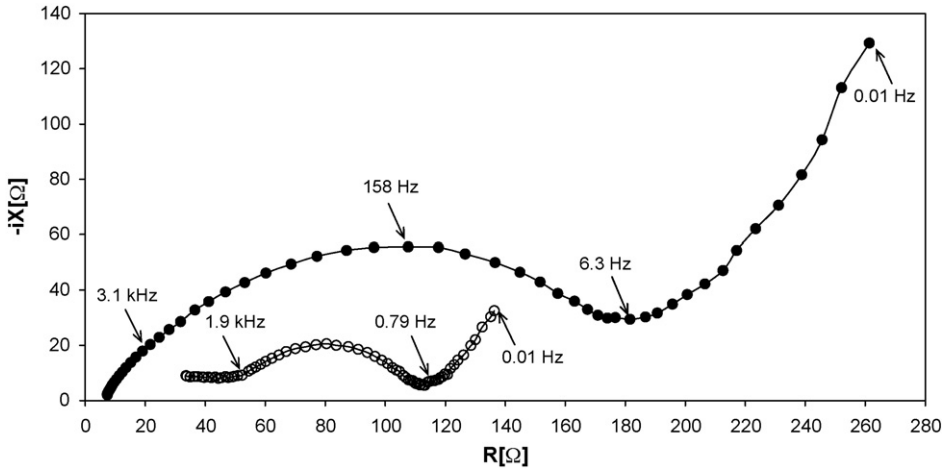

Fig. 7. Impedance plot for the symmetric graphite|0.7 M $LiNTf_2$ in $MePrPyrNTf_2$ + 10 wt.% VC|Li system: (●) fresch cell just after it assembling, (○) recorded after 15 charging/discharging cycles.

recorded just after its assemble, while Fig. 4 shows the corresponding spectrum recorded after 36 days of keeping the cell under open circuit conditions. It can be seen from the impedance plots that when lithium metal is contacted with the $[Li^+][MePrPyr^+][NTf_2^-]$ ionic liquid, the impedance increases considerably with time, by ca. three orders of magnitude. The impedance plots were analyzed according to the equivalent circuit shown in Fig. 5. The ohmic part of the impedance depends on the electrolyte bulk resistance, R_s, the resistance of the film formed between electrolyte and the electrode, R_f, as well on the charge transfer resistance, R_{ct}, at the Li/IL interface. The Warburg resistance (impedance), Z_w, due to Li^+ cation diffusion through the solid film was also taken into account. The analyzed equivalent circuit consists of the electrolyte bulk resistance R_s in series with two sub-circuits. The first sub-circuit represents the film formed at the electrode and consists of the film bulk resistance R_f parallel to its capacity C_f. The second sub-circuit represents the region of the film/electrode interface. The latter sub-circuit consists of the double layer capacity C_{dl} in parallel to the charge transfer resistance R_{ct} and Warburg impedance Z_w. Deconvolution of the impedance plot of the fresh Li/$[Li^+][MePrPyr^+][NTf_2^-]$/Li system (Fig. 3) suggests the R_s resistance at the level of 22 Ω and the resistances of the film and the charge transfer reaction at the comparable level: R_f = 73 Ω and R_{ct} = 78 Ω. However, after 36 days of storage the resistances R_f and R_{ct} increased to 36400 Ω and 82800 Ω, respectively. This suggests that the passivation film formed at the IL/Li interface is very resistive and the rate of the charge transfer reaction is considerably decreased. The evolution of the Li/IL interface impedance, after open circuit conditions, is considerably depressed by the presence of vinylene carbonate in the electrolyte. Fig. 6 shows the impedance plot for the symmetrical system Li/($[Li^+][MePrPyr^+][NTf_2^-]$ + VC)/Li recorded after 34 days of storage (here the electrolyte contained vinylene carbonate as an additive). It can be seen from Fig. 6 that the impedance increased only by one order of magnitude in comparison to the fresh system (Fig. 3). The film bulk resistance and charge transfer resistances determined by the plot deconvolution, increased to 700 Ω and 235 Ω, respectively. Comparison of impedance spectra of the ionic liquid without (Fig. 4) and with VC (Fig. 6) suggests the formation of different type of the passivation film. In the latter case some kind of protective film is formed chemically when the lithium metal is contacted with the ionic liquid containing vinylene carbonate.

Fig. 7 shows the corresponding impedance spectra recorded in the system where one lithium sheet was replaced by the graphite electrode and the G/IL/Li cell was galvanostatically charged and discharged. The initial impedance, recorded just after assembling the cell, decreased after charging the graphite (intercalation with lithium). In the G/($[Li^+][MePrPyr^+][NTf_2^-]$ + VC)/Li cell, the SEI protective coating is formed electrochemically on both electrodes (graphite anode and lithium counter-electrode). After 15 charging/discharging cycles the ohmic resistance did not change considerably. The film bulk resistance, R_f, decreased from the initial 25 Ω to ca. 15 Ω, and at the same time the charge transfer resistance decreased from 200 Ω to ca. 87 Ω. This indicates that the SEI protective coating, formed electrochemically, shows lower bulk resistance as well as increased rate of the charge transfer reaction.

3.4. Galvanostatic charging/discharging

The behaviour of the G/($[Li^+][MePrPyr^+][NTf_2^-]$)/Li cell (the electrolyte does not contain any additive) during galvanostatic charging/discharging is shown in Fig. 8. The intercalation of the graphite is equivalent to the charging capacity of ca. 280 mAh g^{-1}, much less than the maximum theoretical value (ca. 370 mAh g^{-1}). After the first intercalation, the discharging capacity of the graphite is at the level of only 80–90 mAh g^{-1}. However, the charging/discharging properties of the graphite working together with the ionic liquid containing 10 wt.% of VC is close to the maximum theoretical value (Figs. 9–11). The capacity of the first intercalation is at the level of ca. 490 mAh g^{-1}, while the capacity of the first deintercalation is ca. 350 mAh g^{-1}. During the next cycles, the

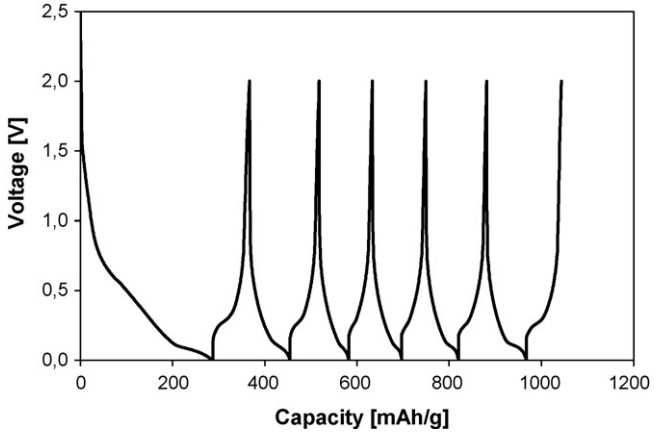

Fig. 8. Galvanostatic charging/discharging of the graphite/0.7 M $LiNTf_2$ in $MePrPyrNTf_2$/Li. Current: 10 mA g^{-1}. Graphite mass in the anode: 4.2 mg.

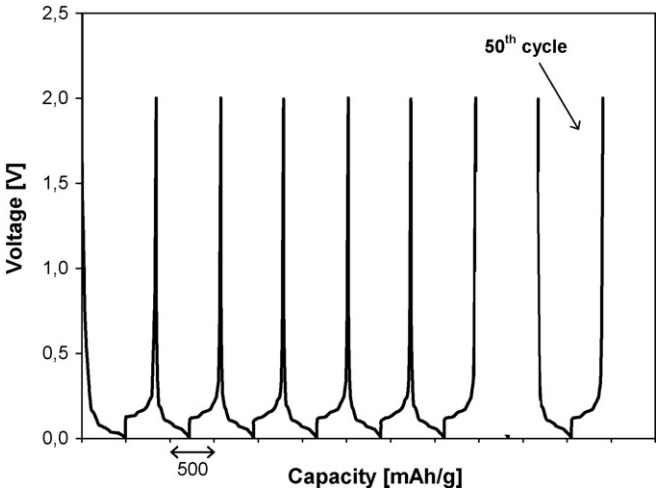

Fig. 9. Galvanostatic charging/discharging of the graphite/0.7 M $LiNTf_2$ in $MePrPyrNTf_2$ + 10 wt.% of VC/Li. Current: 10 mA g^{-1}. Graphite mass in the anode: 4.3 mg.

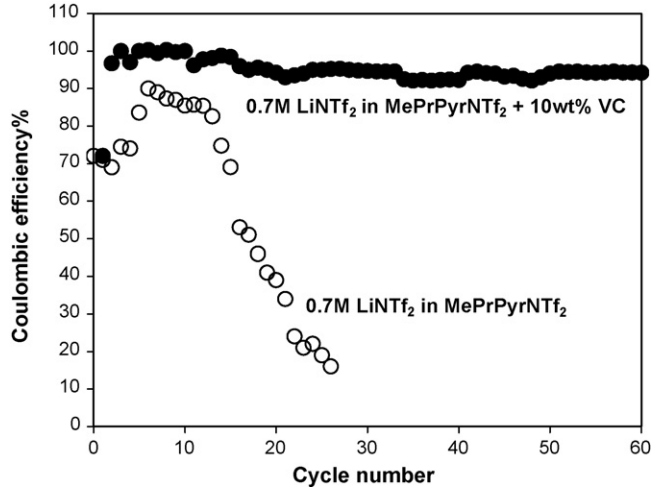

Fig. 10. Coulombic efficiency the graphite anode charging/discharging.

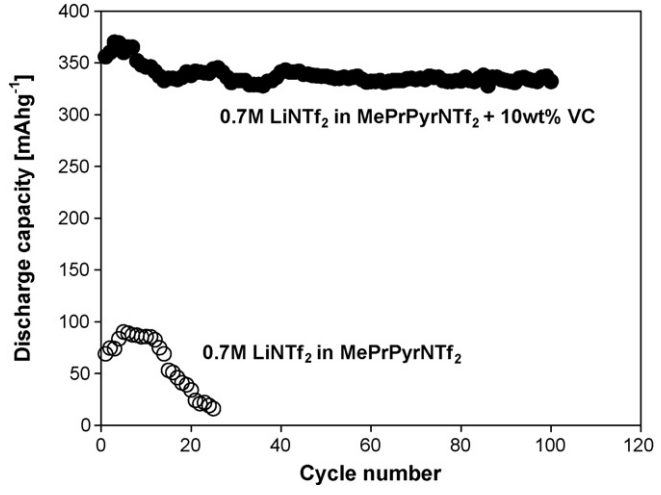

Fig. 11. Discharge capacity of the graphite anode.

capacity of the electrode goes slowly down to stabilize at the level of ca 340 mAh g^{-1} after 50 cycles. The carbon loses its capacity due to the graphite exfoliation during its continuous intercalation and de-intercalation processes, which leads to the degradation of its structure.

4. Conclusions

1. $[Li^+]_{0.09}[MePrPyr^+]_{0.41}[NTf_2{}^-]_{0.50}$ ionic liquid, may be obtained by the dissolution of the solid $LiNTf_2$ salt in the $MePrPyrNTf_2$ salt liquid in room temperature.
2. Lithium metal contacted with the ionic liquid corrodes with the formation of a highly resistive film. The addition of vinylene carbonate to the neat ionic liquid results in the formation of the protective coating (SEI) on both lithium and graphite anodes. The SEI formation increases the rate of the charge transfer reaction as well as protects the anode from chemical passivation (corrosion).
3. The graphite–lithium (C_6Li) anode shows good cyclability and Coulombic efficiency in the presence of 10 wt.% of vinylene carbonate as an additive to the ionic liquid.

Acknowledgement

The work was supported by grant DS31-154/08

References

[1] M. Wakihara, O. Yamamoto (Eds.), Lithium Ion batteries, Wiley–VCH, 1998.
[2] C.A. Vincent, B. Scrosati, Modern Batteries, Wiley, 1997.
[3] F.M. Gray, Solid Polymer Electrolytes, VCH, 1991.
[4] M. Galiński, A. Lewandowski, I. Stępniak, Electrochim. Acta 51 (2006) 5567.
[5] A. Fernicola, B. Scrosati, H. Ohno, Ionics 12 (2006) 95.
[6] K. Xu, S. Zhang, C.A. Angell, J. Electrochem. Soc. 143 (1996) 3548.
[7] H. Sakaebe, H. Matsumoto, Electrochem. Commun. 5 (2003) 594.
[8] H. Nakagawa, S. Izuchi, K. Kuwana, T. Nukuda, Y. Aihara, J. Electrochem. Soc. 150 (2003) A695.
[9] M. Holzapfel, C. Jost, P. Novak, Chem. Commun. (2004) 2098.
[10] M. Egashira, S. Okada, J.-I. Yamaki, D.A. Dri, F. Bonadies, B. Scrosati, J. Power Sources 138 (2004) 240.
[11] B. Garcia, S. Lavallee, G. Perron, C. Michot, M. Armand, Electrochim. Acta 49 (2004) 4583.
[12] T. Sato, T. Maruo, S. Marukane, K. Takagi, J. Power Sources 138 (2004) 253.
[13] A. Chagnes, M. Diaw, B. Carre, P. Willmann, D. Lemordant, J. Power Sources 145 (2005) 82.
[14] S. Kim, Y. Jung, S.-J. Park, J. Power Sources 152 (2005) 272.
[15] M. Holzapfel, C. Jost, A. Prodi-Schwab, F. Krumeich, A. Wursig, H. Buqa, P. Novak, Carbon 43 (2005) 1488.
[16] J.-H. Shin, W.A. Henderson, G.B. Appetecchi, F. Alessandrini, S. Passerini, Electrochim. Acta 50 (2005) 3859.
[17] H. Sakaebe, H. Matsumoto, K. Tatsumi, J. Power Sources 146 (2005) 693.
[18] T. Kuboki, T. Okuyama, T. Ohsaki, N. Takami, J. Power Sources 146 (2005) 766.
[19] H. Matsumoto, H. Sakaebe, K. Tatsumi, J. Power Sources 146 (2005) 45.
[20] S.-Y. Lee, H.H. Yong, S.K. Kim, J.Y. Kim, S. Ahn, J. Power Sources 146 (2005) 732.
[21] Y. Zhang, M. Urquidi-Macdonald, J. Power Sources 144 (2005) 191.
[22] M. Diaw, A. Chagnes, B. Carre, P. Willmann, D. Lemordant, J. Power Sources 146 (2005) 682.
[23] H. Zheng, H. Zhang, Y. Fu, T. Abe, Z. Ogumi, J. Phys. Chem. B 109 (2005) 13676.
[24] K. Hayashi, Y. Nemoto, K. Akuto, Y. Sakurai, J. Power Sources 146 (2005) 689.
[25] S.-Y. Lee, H.H. Yong, Y.J. Lee, S.K. Kim, S. Ahn, J. Phys. Chem. B 109 (2005) 13663.
[26] H. Zheng, J. Qin, Y. Zhao, T. Abe, Z. Ogumi, Solid State Ionics 176 (2005) 2219.
[27] S. Seki, Y. Kobayashi, H. Miyashiro, Y. Ohno, Y. Mita, A. Usami, N. Terada, M. Watanabe, Electrochem. Solid State 8 (2005) A577.
[28] H. Zheng, K. Jiang, T. Abe, Z. Ogumi, Carbon 44 (2006) 203.
[29] J.S. Lee, N.D. Quan, J.M. Hwang, J.Y. Bae, H. Kim, B.W. Cho, H.S. Kim, H. Lee, Electrochem. Commun. 8 (2006) 460.
[30] M. Egashira, M. Tanaka-Nakagawa, I. Watanabe, S. Okada, J. Yamaki, J. Power Sources 160 (2006) 1387.
[31] M. Ishikawa, T. Sugimoto, M. Kikuta, E. Ishiko, M. Kono, J. Power Sources 162 (2006) 658.
[32] Y. Abu-Lebdeh, A. Abouimrane, P.-J. Alarco, M. Armand, J. Power Sources 154 (2006) 255.
[33] E. Markevich, V. Baranchugov, D. Aurbach, Electrochem. Commun. 8 (2006) 1331.
[34] H. Matsumoto, H. Sakaebe, K. Tatsumi, M. Kikuta, E. Ishiko, M. Kono, J. Power Sources 160 (2006) 1308.
[35] J. Xu, J. Yang, Y. NuLi, J. Wang, Z. Zhang, J. Power Sources 160 (2006) 621.
[36] L.X. Yuan, J.K. Feng, X.P. Ai, Y.L. Cao, S.L. Chen, H.X. Yang, Electrochem. Commun. 8 (2006) 610.

[37] J.-H. Shin, W.A. Henderson, S. Scaccia, P.P. Prosini, S. Passerini, J. Power Sources 156 (2006) 560.
[38] S. Seki, Y. Kobayashi, H. Miyashiro, Y. Ohno, A. Usami, J. Mita, M. Watanabe, N. Terada, Chem. Commun. (2006) 544.
[39] S. Seki, Y. Kobayashi, H. Miyashiro, Y. Ohno, A. Usami, Y. Mita, N. Kihira, M. Watanabe, N. Terada, J. Phys. Chem. B 110 (2006) 10228.
[40] H. Zheng, B. Li, Y. Fu, T. Abe, Z. Ogumi, Electrochim. Acta 52 (2006) 1556.
[41] A. Lewandowski, A. Swiderska-Mocek, J. Power Sources 171 (2007) 938.
[42] J.-W. Choi, G. Cheruvally, Y.-H. Kim, J.-K. Kim, J. Manuel, P. Raghavan, J.-H. Ahn, K.-W. Kim, H.-J. Ahn, D.S. Choi, C.E. Song, Solid State Ionics 178 (2007) 1235.
[43] Y.-H. Kim, G. Cheruvally, J.W. Choi, J.H. Ahn, K.W. Kim, H.J. Ahn, D.S. Choi, C.E. Song, Macromol. Symp. 249–250 (2007) 183.
[44] D.M. Tigelaar, M.A.B. Meador, W.R. Bennett, Macromolecules 40 (2007) 4159.
[45] G. Cheruvally, J.-K. Kim, J.-W. Choi, J.-H. Ahn, Y.-J. Shin, J. Manuel, P. Raghavan, K.-W. Kim, H.-J. Ahn, D.S. Choi, C.E. Song, J. Power Sources 172 (2007) 863.
[46] G.T. Kim, G.B. Appetecchi, F. Alessandrini, S. Passerini, J. Power Sources 171 (2007) 861.
[47] V. Baranchugov, E. Markevich, E. Pollak, G. Salitra, D. Aurbach, Electrochem. Commun. 9 (2007) 796.
[48] S. Seki, Y. Mita, H. Tokuda, Y. Ohno, Y. Kobayashi, A. Usami, M. Watanabe, N. Terada, H. Miyashiro, Electrochem. Solid State 10 (2007) A237.
[49] S. Seki, Y. Ohno, Y. Kobayashi, H. Miyashiro, A. Usami, Y. Mita, H. Tokuda, M. Watanabe, K. Hayamizu, S. Tsuzuki, M. Hattori, N. Terada, J. Electrochem. Soc. 154 (2007) A173.
[50] Y. Kobayashi, Y. Mita, S. Seki, Y. Ohno, H. Miyashiro, N. Terada, J. Electrochem. Soc. 154 (2007) A677.
[51] H. Nakagawa, Y. Fujino, S. Kozono, Y. Katayama, T. Nukuda, H. Sakaebe, H. Matsumoto, K. Tatsumi, J. Power Sources 174 (2007) 1021.
[52] A. Fernicola, F. Croce, B. Scrosati, T. Watanabe, H. Ohno, J. Power Sources 174 (2007) 342.
[53] L. Zhao, J.-i. Yamaki, M. Egashira, J. Power Sources 174 (2007) 352.
[54] M. Egashira, H. Todo, N. Yoshimoto, M. Morita, J.-I. Yamaki, J. Power Sources 174 (2007) 560.
[55] H. Ye, J. Huang, J.J. Xu, A. Khalfan, S.G. Greenbaum, J. Electrochem. Soc. 154 (2007) A1048.
[56] A. Guerfi, S. Duchesne, Y. Kobayashi, A. Vijh, K. Zaghib, J. Power Sources 175 (2008) 866.
[57] D.-W. Kim, S.R. Sivakkumar, D.R. MacFarlane, M. Forsyth, Y.-K. Sun, J. Power Sources 180 (2008) 591.
[58] H. Sakaebe, H. Matsumoto, K. Hironori, Y. Miyazaki, Patent JP2003331918, (2003).
[59] S. Passerini, W. A. Henderson, J-H. Shin, F. Alessandrini, Patent US20050287441, (2005).
[60] A. Lewandowski, M. Osinska, A. Swiderska-Mocek, M. Galinski, Electroanalysis 20 (2008) 1903.